RSC Advances

PAPER

View Article Online
View Journal | View Issue

Cite this: *RSC Adv.*, 2022, **12**, 13261

Study of resistance performance of Al_2O_3–ZnO–Y_2O_3 thermal control coating exposed to vacuum-ultraviolet irradiation

Tao Li,[a] Hongjun Kang,[a] Songtao Lu,*[a] Wei Qin [b] and Xiaohong Wu *[a]

As deep space exploration moves farther and farther away, thermal control coating of the in-orbit spacecraft will suffer a serious vacuum-ultraviolet radiation environment, which seriously threatens the reliability of the spacecraft in orbit. Therefore, it is important to improve the vacuum-ultraviolet resistance performance of the thermal control coating. In this work, the inorganic Al_2O_3–ZnO–Y_2O_3 thermal control coating was *in situ* fabricated on a 6061 aluminum alloy surface by PEO technology, and its vacuum-ultraviolet resistance performance was investigated. The results show that the Al_2O_3–ZnO–Y_2O_3 thermal control coating has a good resistance performance to vacuum-ultraviolet radiation, which is mainly because the large extinction coefficients of the ZnO and Y_2O_3 materials in the ultraviolet band are conducive to improving the ultraviolet resistance performance. Furthermore, the life prediction model of the Al_2O_3–ZnO–Y_2O_3 thermal control coating shows that its $\Delta\alpha_s$ value first slightly increases and then tends to be stable with the increase of ultraviolet irradiation time from 0 ESH to 25 000 ESH, and the maximum variation of $\Delta\alpha_s$ is about 0.0536. This work provides a material basis and technical support for the thermal control system of spacecraft with long life and high reliability.

Received 10th January 2022
Accepted 2nd April 2022

DOI: 10.1039/d2ra00167e

rsc.li/rsc-advances

1. Introduction

With the development of space science and technology, geosynchronous orbit satellites are being developed with light weight, long life and high reliability.[1,2] Thermal control coating is a main passive thermal control means to ensure the temperature balance of the satellite,[3–5] guaranteeing the highly reliable operation of the satellite. Therefore, it is desired to develop a novel thermal control coating with light weight and high space stability to improve the service life of satellites.

At present, thermal control coatings are mainly divided into organic coatings and inorganic coatings according to composition.[6] In particular, inorganic thermal control coatings have a low radiation–absorption ratio and excellent stability in the space environment, which is preferred for spacecraft cooling surface at present.[7,8] Because the thermal control coating is located on the outer surface of the spacecraft, it will be directly exposed to the harsh space environments, such as high vacuum, charged particles, ultraviolet radiation, atomic oxygen and so on.[9–12] Among the harsh space environments, it is worth noting that the vacuum-ultraviolet radiation will cause the serious degradation of thermal control performance and affect its function because high-energy UV photons can cause "color center" generation on the inorganic thermal control coating surface.[13] Thus, it is important to improve vacuum-ultraviolet resistance performance of inorganic thermal control coating.

Zinc oxide (ZnO), as excellent ultraviolet resistant material,[14] which is widely chosen to prepare the inorganic thermal control coating of spacecraft because of the matching between band gap width and ultraviolet wavelength, chemical stability at high temperature, and permanent stability under UV exposure. Meanwhile, studies have found that rare earth modified ZnO-based micro-arc oxidation coating can effectively reduce the UV absorption capacity,[15] and Y_2O_3 exhibits unique electrical, magnetic and chemical properties due to their unique electronic structure, which can inhibit the crystal phase transition of metal oxides,[16,17] and thus improve the stability of thermal control coating. Accordingly, introducing ZnO and Y_2O_3 into the inorganic thermal control coating can drastically improve its vacuum-ultraviolet resistance performance.

Herein, in this work, an inorganic Al_2O_3–ZnO–Y_2O_3 thermal control coating was *in situ* fabricated on the 6061 aluminum alloy surface by plasma electrolytic oxidation (PEO) technology. The vacuum-ultraviolet resistance performance of Al_2O_3–ZnO–Y_2O_3 thermal control coating was investigated by testing and analyzing its thermal control performance, mass loss ratio, surface microstructure and phase structure before and after vacuum-ultraviolet irradiation 2000 ESH. Furthermore, the life

[a]*MIIT Key Laboratory of Critical Materials Technology for New Energy Conversion and Storage, School of Chemistry and Chemical Engineering, Harbin Institute of Technology, Harbin, Heilongjiang 150001, PR China. E-mail: lusongtao@hit.edu.cn; wuxiaohong@hit.edu.cn*

[b]*National Key Laboratory of Materials Behavior and Evaluation Technology in Space Environment, School of Materials Science and Engineering, Harbin Institute of Technology, Harbin, Heilongjiang 150001, China*

prediction model of Al_2O_3–ZnO–Y_2O_3 thermal control coating under vacuum-ultraviolet irradiation is preliminarily established. This work provides a material basis and technical support for the thermal control system of spacecraft with long life and high reliability.

2. Experimental

2.1 Materials

Sodium polyphosphate ($Na_2H_2P_2O_7$), sodium metasilicate (Na_2SiO_3), zinc dihydrogen phosphate ($Zn(H_2PO_4)_2$) and ethylenediamine tetraacetic acid disodium salt (Na_2EDTA) were provided by Tianjin Chemical Reagent Company, China. Yttrium nitrate ($Y(NO_3)_2$) and potassium hydroxide (KOH) were purchased from Aladdin Reagent Company. Other chemical reagents were supplied by Harbin local reagent company. All reagents were analytical grade and used without further purification.

2.2 Preparation of Al_2O_3–ZnO–Y_2O_3 thermal control coating

Al_2O_3–ZnO–Y_2O_3 thermal control coating was fabricated on the 6061 aluminum alloy surface with a dimension of 4 cm × 4 cm × 0.2 cm by plasma electrolytic oxidation (PEO) technology. Prior to the PEO treatment, aluminum alloy surface was polished by using 150, 400 and 800 mesh abrasive paper, respectively, and ultrasonically degreased in acetone and then cleaned with the distilled water. The 20 kW bipolar pulsed power supply was employed to carry out the PEO reaction of the samples in the electrobath of the stainless steel serving as the cathode.[18,19] The power parameters were fixed at the pulse frequency of 500 Hz, the current density of 10 A dm^{-2}, the duty ratio of 30% and oxidation time of 15 min. The electrolyte solution consists of 30 g L^{-1} $Na_2H_2P_2O_7$, 20 g L^{-1} Na_2SiO_3, 10 g L^{-1} $Zn(H_2PO_4)_2$, 10 g L^{-1} Na_2EDTA, 8 g L^{-1} KOH and 6 g L^{-1} $Y(NO_3)_3 \cdot 6H_2O$. After the PEO process, the obtained samples were rinsed with water and then dried in the air.

2.3 Simulation experiment of vacuum-ultraviolet irradiation

The vacuum-ultraviolet irradiation simulation experiment in space of Al_2O_3–ZnO–Y_2O_3 thermal control coating on the aluminum alloy surface was operated in the near ultraviolet irradiation area under the power of 1000 W mercury xenon lamp with the infrared and visible light filter, and the test related parameters mainly include the vacuum degree below 1×10^{-5} Pa, irradiance of 4 SC, sample temperature of 30 °C and heat sink temperature below −35 °C. The vacuum-ultraviolet irradiation amount is 500–2000 ESH (equivalent solar hour: the total irradiation amount corresponding to the sample irradiated for 1 hour with a solar constant),[20] and the solar absorptivity (α_s) and emissivity (ε) of the selected sample before and after vacuum-ultraviolet irradiation were measured to evaluate the vacuum-ultraviolet resistance performance through an *in situ* measurement system in the equipment.

2.4 Characterization

The coating thickness of the Al_2O_3–ZnO–Y_2O_3 thermal control coating was measured through the coating thickness gauge (TT260, Beijing Times Peak Technology Co., Ltd). The microstructure of Al_2O_3–ZnO–Y_2O_3 thermal control coating was observed by scanning electron microscope (SEM, Hitachi, S-570). 3D surface structure was measured by atomic force microscope (AFM, CSPM 5500). The crystal structure of Al_2O_3–ZnO–Y_2O_3 thermal control coating was characterized by X-ray diffractometer (XRD, Rigaku, Dmax-3B) with a Cu Kα radiation ($\lambda = 1.54060$ Å). The emissivity (ε) at 2–16 μm was examined by an infrared reflectometer (Gier-Dunkle DB-100) and the solar absorptivity (α_s) in the 200–2500 nm was measured by a UV-VIS-NIR spectrophotometer (PerkinElmer Lambda 950) with an integrating sphere.

3. Result and discussion

3.1 Thermal control performance

As we all know, the coating thickness plays an important role in its thermal control performance. Under the condition of satisfying the requirements of thermal control performance of spacecraft, weight reduction of spacecraft still needs to be considered. Therefore, in this work, the thickness of the as-prepared Al_2O_3–ZnO–Y_2O_3 thermal control coating is controlled at about 30 μm. According to the test method B-Cross-Cut tape test of ASTM-D3359-17 standard, the classification of adhesion test results for the obtained Al_2O_3–ZnO–Y_2O_3 thermal control coating is 5B. Fig. 1 is the emissivity and absorptivity variation of Al_2O_3–ZnO–Y_2O_3 thermal control coating at different vacuum-ultraviolet irradiation time. As shown in Fig. 1, it can be seen that the initial emissivity and absorptivity of the Al_2O_3–ZnO–Y_2O_3 thermal control coating are 0.859 and 0.405, respectively, which meet the application requirements. With the increase of vacuum-ultraviolet irradiation time from 0 ESH to 2000 ESH, its emissivity cannot decrease but slightly increase from 0.859 to 0.878 (Fig. 1a), indicating that the vacuum-ultraviolet irradiation has no adverse effect on the emissivity of Al_2O_3–ZnO–Y_2O_3 thermal control coating. On contrast, although its absorptivity also presents a slight increase from 0.405 to 0.435 (Fig. 1b) and the variation is very little, which can still meet the application requirements. The above results show that vacuum-ultraviolet irradiation has little effect on thermal control performance of Al_2O_3–ZnO–Y_2O_3 thermal control coating.

3.2 Mass loss ratio

The mass loss ratio variation of Al_2O_3–ZnO–Y_2O_3 thermal control coating on aluminum alloy surface under different vacuum-ultraviolet irradiation time is shown in Fig. 2. It can be seen that the mass loss ratio of Al_2O_3–ZnO–Y_2O_3 thermal control coating shows an increase trend within the vacuum-ultraviolet irradiation time of 1000 ESH, which is attributed to the precipitation of adsorbed impurities and degradation product.[21] Continuing to increase the vacuum-ultraviolet irradiation time from 1000 ESH to 2000 ESH, its mass loss ratio basically maintains a stable value of about 0.50 mg cm^{-2}, which can meet the requirements of mass loss for spacecraft thermal control coating, indicating that Al_2O_3–ZnO–Y_2O_3 thermal

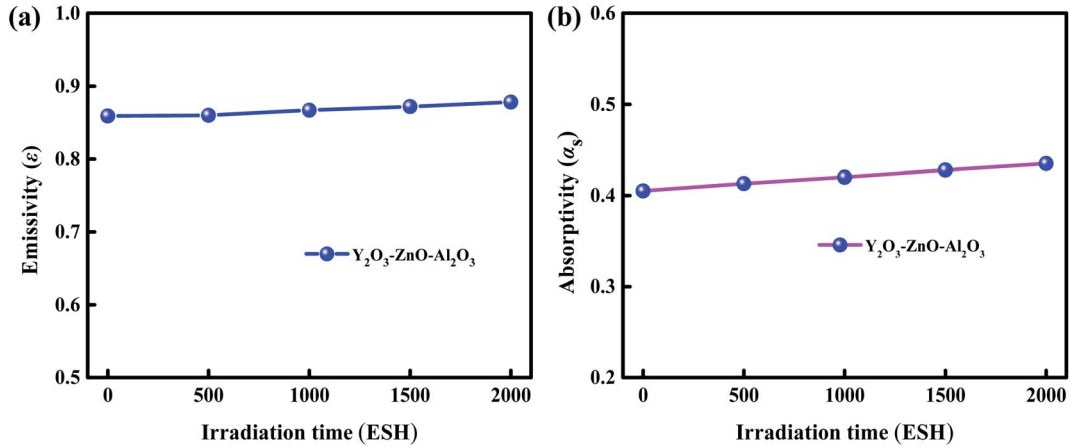

Fig. 1 The emissivity (a) and absorptivity (b) variation of Al_2O_3–ZnO–Y_2O_3 thermal control coating at different vacuum-ultraviolet irradiation time.

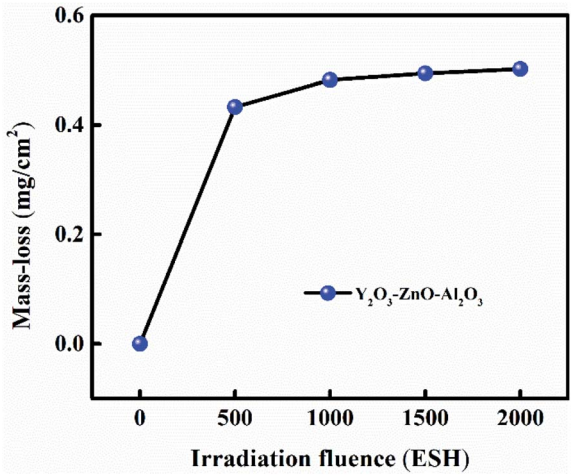

Fig. 2 The variation of mass loss ratio for the Al_2O_3–ZnO–Y_2O_3 thermal control coating.

control coating has a good stability in vacuum-ultraviolet environment.

3.3 Surface morphology analysis

In order to investigate the effect of vacuum-ultraviolet irradiation on surface morphology of Al_2O_3–ZnO–Y_2O_3 thermal control coating, SEM and AFM were used to observe the surface morphology variation of Al_2O_3–ZnO–Y_2O_3 thermal control coating before and after vacuum-ultraviolet irradiation 2000 ESH, as shown in Fig. 3. It can be seen that the surface morphology of Al_2O_3–ZnO–Y_2O_3 thermal control coating cannot be changed after vacuum-ultraviolet irradiation 2000 ESH, indicating that the surface morphology of thermal control coating has a good stability under vacuum-ultraviolet irradiation.

3.4 Phase structure analysis

The phase structure variation of Al_2O_3–ZnO–Y_2O_3 thermal control coating can be determined by XRD measurement. Fig. 4 is XRD patterns of Al_2O_3–ZnO–Y_2O_3 thermal control coating before and after vacuum-ultraviolet irradiation 2000 ESH. It can be seen that the main diffraction peaks location of Al_2O_3–ZnO–Y_2O_3 thermal control coating before and after vacuum-ultraviolet irradiation 2000 ESH cannot be changed, indicating that the phase structure of thermal control coating also has a good stability under vacuum-ultraviolet irradiation.

3.5 Vacuum-ultraviolet resistance mechanism

From the analysis of atomic structure, when the ultraviolet photon irradiates the Al_2O_3–ZnO–Y_2O_3 thermal control coating, the electrons around the lattice atoms at the irradiation will generate the deviation. When the deviation is accumulated to a certain extent, the spectral absorption effect will be generated, causing the increase of the absorption ratio (α_s). The number of lattices without color center, the number of existing color center lattices and ultraviolet irradiation were positively correlated with the negative exponent of the product of color center formation probability and incident intensity. The material is considered to be an ideal material. The lattice number of color center generation in each molecular layer is N_0, and the probability of color center generation in the inner molecular layer is μ. Therefore, the relation between color center concentration (C_d) and irradiation time (T), color center generation probability is shown in formula (1).

$$C_d = \frac{N(X,T)}{N_0} = 1 - \exp[-T\mu\exp(-BX)] \quad (1)$$

where X is penetration depth of ultraviolet irradiation photons, and B is the wavelength absorption coefficient of the thermal control coating in the ultraviolet band region. According to the above formula (1), there are the two limiting conditions with the change of irradiation time: (1) when $T = 0$, $N(X, T) = 0$, $C_d = 0$, $\alpha_s(T)$ is the initial value α_0; (2) when $T \to \infty$, $N(X, T) \to N_0$, $C_d \to 1$, $\alpha_s(T)$ tends to the limit value α_U. Based on above two limit conditions, formula (1) was integrated to obtain the formula (2).

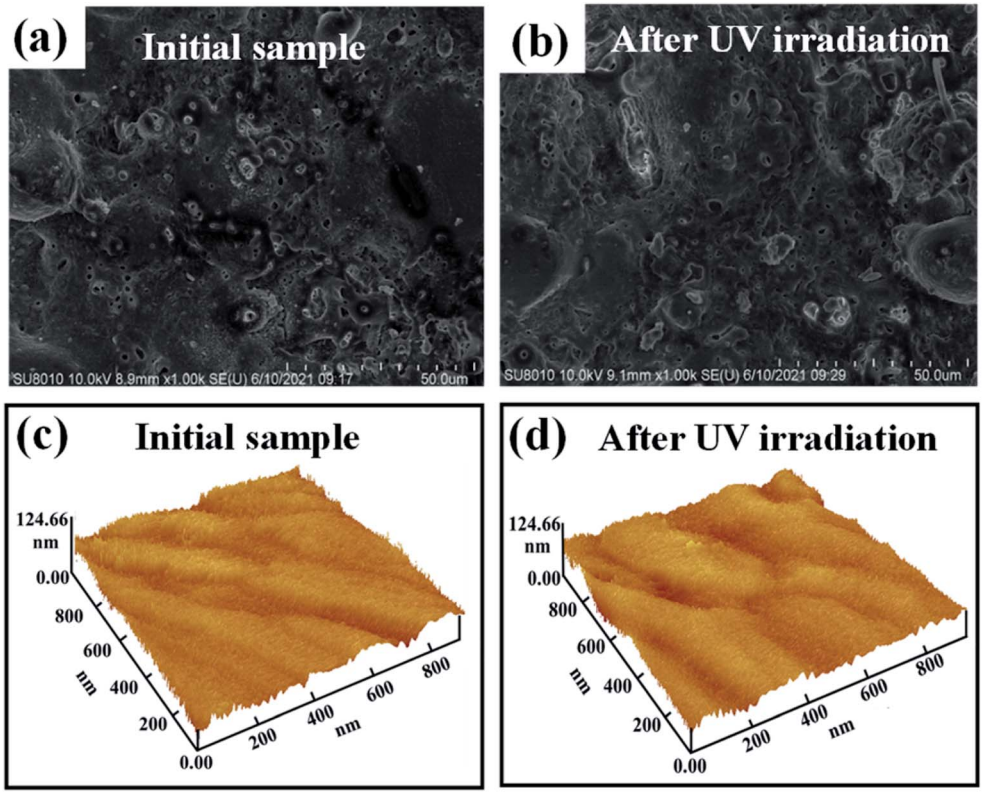

Fig. 3 SEM (a) and (b) and AFM images (c) and (d) of Al_2O_3–ZnO–Y_2O_3 thermal control coating before and after vacuum-ultraviolet irradiation 2000 ESH.

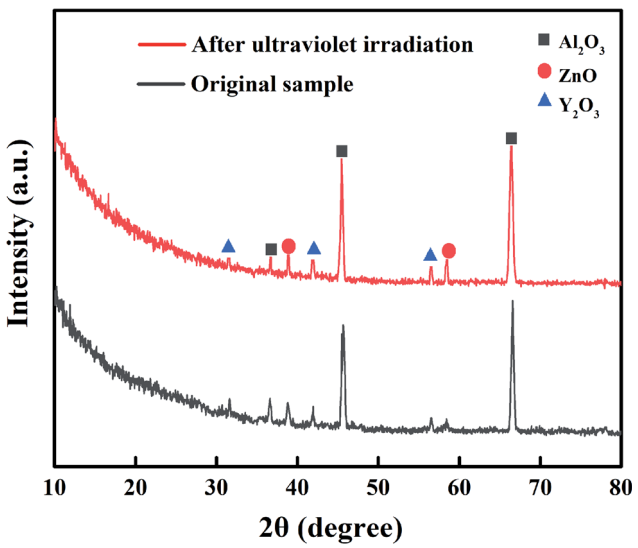

Fig. 4 XRD patterns of Al_2O_3–ZnO–Y_2O_3 thermal control coating before and after vacuum-ultraviolet irradiation 2000 ESH.

$$\alpha_s(T) = \alpha_0 \int_0^D \frac{N_0 - N(X,T)}{N_0} dX + \alpha_U \int_0^D \frac{N(X,T)}{N_0} dX \quad (2)$$

where D is the total thickness of the thermal control coating. Since ultraviolet irradiation has a threshold of penetration depth d_U, the formula (2) can be transformed into the following formula (3), and thus a mathematical model of solar absorption degradation of thermal control coatings under ultraviolet irradiation can be obtained.

$$\Delta\alpha_s(T) = D^{-1}(\alpha_U - \alpha_0) \int_0^{d_U} \{1 - \exp[-T\mu I_0 \exp(-BX)]\} dX \quad (3)$$

According to the formula (3), it can be seen that $\Delta\alpha_s(T)$ is related to ultraviolet extinction coefficient of thermal control coating when the external environment, ultraviolet irradiation intensity and time are fixed. Therefore, the material with a large extinction coefficient in the ultraviolet band is conducive to improving the ultraviolet irradiation resistance of the

Table 1 The absorptivity variation ($\Delta\alpha_s$) of Al_2O_3–ZnO–Y_2O_3 thermal control coating

Ultraviolet irradiation time (ESH)	After ultraviolet irradiation α_S	Variation $\Delta\alpha_S$
0	0.405	0
500	0.414	+0.009
1000	0.423	+0.018
1500	0.427	+0.022
2000	0.434	+0.029
3000	0.441	+0.036
4000	0.446	+0.041
5000	0.451	+0.046

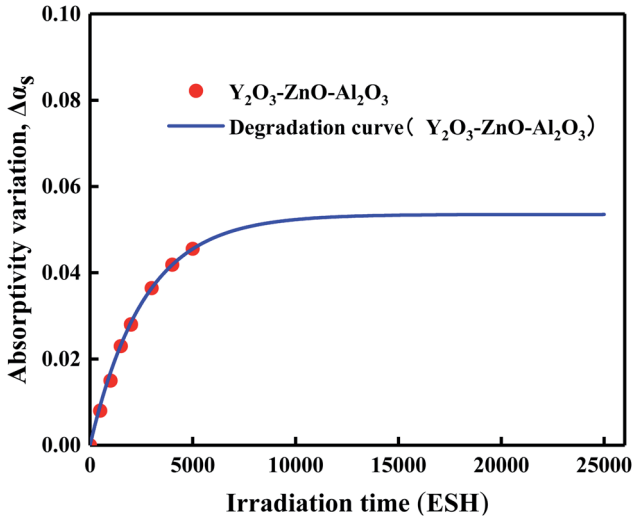

Fig. 5 The prediction $\Delta\alpha_s$ degradation curve of Al_2O_3–ZnO–Y_2O_3 thermal control coating under vacuum-ultraviolet irradiation.

thermal control coating. Therefore, because the ZnO and Y_2O_3 materials have the large extinction coefficients in the ultraviolet band, the prepared Al_2O_3–ZnO–Y_2O_3 thermal control coating has excellent resistance performance exposed to the ultraviolet irradiation.

3.6 Service life prediction model

In order to study the degradation of thermal radiation characteristics of thermal Al_2O_3–ZnO–Y_2O_3 control coating under space UV irradiation, ultraviolet irradiation evaluation test of thermal control coating was carried out by ground irradiation simulation equipment, and the absorption ratio of thermal control coating under different irradiation time was measured by *in situ* test method. Table 1 is the absorptivity variation ($\Delta\alpha_s$) of Al_2O_3–ZnO–Y_2O_3 thermal control coating, and the $\Delta\alpha_s$ test data were fitted to obtain the service life prediction model of solar absorption degradation under ultraviolet irradiation to better understand the α_s degradation law of Al_2O_3–ZnO–Y_2O_3 thermal control coating under ultraviolet irradiation. Fig. 5 shows the prediction $\Delta\alpha_s$ degradation curve of Al_2O_3–ZnO–Y_2O_3 thermal control coating under vacuum-ultraviolet irradiation.

The experimental data fitting results show that the prediction $\Delta\alpha_s$ degradation model of Al_2O_3–ZnO–Y_2O_3 thermal control coating are exponential functions,[22] as shown in formula (4).

$$\Delta\alpha_s = 0.05356 - 0.03988 \exp\left(-\frac{T}{2631.579}\right) \quad (4)$$

According to the research, the total ultraviolet radiation received by the synchronous orbit spacecraft in 3 years is about 25 000 ESH.[23] It can be seen from the above formula (4) that when the ultraviolet irradiation time less 7000 ESH, the $\Delta\alpha_s$ of Al_2O_3–ZnO–Y_2O_3 thermal control coating is only 0.0536. When the increase of ultraviolet irradiation time from 7000 ESH to 25 000 ESH, its $\Delta\alpha_s$ tends to be stable value, indicating that Al_2O_3–ZnO–Y_2O_3 thermal control coating has a good resistance performance to vacuum-ultraviolet radiation.

4. Conclusion

The inorganic Al_2O_3–ZnO–Y_2O_3 thermal control coating was *in situ* fabricated on the 6061 aluminum alloy surface by PEO technology. The vacuum-ultraviolet resistance performance of Al_2O_3–ZnO–Y_2O_3 thermal control coating was investigated. The results show that Al_2O_3–ZnO–Y_2O_3 thermal control coating has good resistance performance to vacuum-ultraviolet irradiation, which is mainly because the large extinction coefficients of ZnO and Y_2O_3 materials in the ultraviolet band is conducive to improve the vacuum-ultraviolet resistance performance. Furthermore, the life prediction model of Al_2O_3–ZnO–Y_2O_3 thermal control coating shows that its $\Delta\alpha_s$ is only 0.536 under vacuum-ultraviolet irradiation time less than 7000 ESH, and then its $\Delta\alpha_s$ tends to be stable value with the increase of ultraviolet irradiation time from 7000 ESH to 25 000 ESH. This work provides a material basis and technical support for the thermal control system of spacecraft with long life and high reliability.

Author contributions

Tao Li and Hongjun Kang are roles for conceptualization, investigation, writing-original draft. Songtao Lu is role for investigation and validation. Wei Qin and Xiaohong Wu are role for resources and data curation.

Conflicts of interest

There are no conflicts to declare.

Acknowledgements

This work was financially supported by the National Natural Science Foundation of China (No. U2067216, U2130109 and 51902070).

Notes and references

1 Z. W. Qin, L. Wang, G. W. Huang, Q. Zhang, X. Y. Yan, S. C. Xie, H. N. She, F. Yue and X. L. Wang, *Remote Sens.*, 2021, **13**, 629–647.
2 C. Liu, W. G. Gao, B. Shao, J. Lu, W. Wang, Y. Chen, C. G. Su, S. Xiong and Q. Ding, *Navigation*, 2021, **68**, 405–417.
3 H. W. Babel, C. Jones and K. David, *Acta Astronaut.*, 1996, **39**, 369–379.
4 Z. Y. Du, M. Li, S. C. Xu, K. B. Li, F. X. Zou, R. R. Zhang and G. H. Li, *J. Alloys Compd.*, 2022, **895**, 162679–162687.
5 X. Y. Wang, P. F. Ju, X. P. Lu, Y. Chen and F. H. Wang, *Ceram. Int.*, 2022, **48**, 3615–3627.
6 S. Wijewardane and D. Y. Goswami, *Renewable Sustainable Energy Rev.*, 2012, **16**, 1863–1873.
7 K. Tokesi, R. J. Bereczky and I. Rajta, *Nucl. Instrum. Methods Phys. Res., Sect. B*, 2015, **354**, 1–2.

8 N. Kayhan, R. S. Razavi and S. Choopani, *Prog. Org. Coat.*, 2012, **74**, 603–607.
9 G. Bitettia, M. Marchettia, S. Miletia, F. Valentea and S. Scaglione, *Acta Astronaut.*, 2007, **60**, 166–174.
10 V. E. Skurat, E. A. Barbashev, Y. I. Dorofeev, A. P. Nikiforov, M. M. Gorelova and A. I. Pertsyn, *Appl. Surf. Sci.*, 1996, **92**, 441–446.
11 Z. Zang, S. Gu, L. Shi and Z. Wu, *Chin. J. Space Sci.*, 1998, **18**, 342–347.
12 K. B. Shin, C. G. Kim, C. S. Hong and H. H. Lee, *Composites, Part B*, 2000, **31**, 223–235.
13 D. Q. Peng, W. Qin and X. H. Wu, *Acta Astronaut.*, 2015, **11**, 84–88.
14 C. Li, J. Lv, Z. Liang and S. Yao, *Opt. Mater.*, 2013, **35**, 586–589.
15 M. Khuili, N. Fazouan, H. Abou El Makarim, E. H. Atmani, D. P. Rai and M. Houmad, *Vacuum*, 2020, **181**, 109603–109612.
16 B. Gwalani, M. Song, J. Silverstein, J. Escobar, T. H. Wang, M. Pole, K. Johnson, B. K. Jasthi, A. Devaraj and K. Ross, *Scr. Mater.*, 2022, **207**, 114281–114291.
17 A. Ćirić and S. Stojadinović, *J. Lumin.*, 2020, **217**, 116762–116773.
18 H. N. Vatan, R. Ebrahimi-kahrizsangi and M. Kasiri-asgarani, *J. Alloys Compd.*, 2016, **683**, 241–255.
19 X. Y. Wang, X. P. Lu, P. F. Ju, Y. Chen, T. Zhang and F. H. Wang, *Surf. Coat. Technol.*, 2020, **393**, 125709–125723.
20 H. Gao, X. Lan, L. W. Liu, X. L. Xiao, Y. J. Liu and J. S. Leng, *Smart Mater. Struct.*, 2017, **26**, 095001–095014.
21 M. M. Mikhailov and M. L. Dvoretskll, *J. Adv. Mater.*, 1995, **2**, 41–49.
22 T. Liu, Q. Sun, J. Meng, Z. Q. Pan and Y. Z. Tang, *Sol. Energy*, 2016, **139**, 467–474.
23 A. K. Sharma and N. Sridhara, *Adv. Space Res.*, 2012, **50**, 1411–1424.